

## LA-UR-15-25134

Approved for public release; distribution is unlimited.

Title: Validation of MCNP6 for Electron Energy Deposition in Extended Media

Author(s): Dixon, David A.  
Hughes, Henry Grady III

Intended for: 2015 ANS Winter Meeting and Nuclear Technology Expo,  
2015-11-08/2015-11-12 (Washington D. C., District Of Columbia, United  
States)

Issued: 2015-07-20 (rev.1)

---

**Disclaimer:**

Los Alamos National Laboratory, an affirmative action/equal opportunity employer, is operated by the Los Alamos National Security, LLC for the National Nuclear Security Administration of the U.S. Department of Energy under contract DE-AC52-06NA25396. By approving this article, the publisher recognizes that the U.S. Government retains nonexclusive, royalty-free license to publish or reproduce the published form of this contribution, or to allow others to do so, for U.S. Government purposes. Los Alamos National Laboratory requests that the publisher identify this article as work performed under the auspices of the U.S. Department of Energy. Los Alamos National Laboratory strongly supports academic freedom and a researcher's right to publish; as an institution, however, the Laboratory does not endorse the viewpoint of a publication or guarantee its technical correctness.

## Validation of MCNP6 for Electron Energy Deposition in Extended Media

D. A. Dixon,\* H. Grady Hughes\*

\*Los Alamos National Laboratory, P.O. Box 1663, Los Alamos, NM 87545  
ddixon@lanl.gov, hgh@lanl.gov

### INTRODUCTION

The MCNP6 code system [1] has benefited from an extensive program of verification and validation [2], especially in areas such as criticality [3], reactor physics, neutron shielding [4], and other related applications. However, validation of the MCNP6 electron-photon transport algorithms has been more limited [5, 6, 7]. Therefore, it is of interest to extend the electron transport validation efforts to include a wider range of experimental benchmarks. An extended validation will demonstrate the range of validity of the electron transport algorithms when calculating quantities such as energy deposition, charge deposition, angular distributions, energy spectra, reflection and transmission coefficients, and bremsstrahlung.

This paper summarizes a preliminary energy deposition validation study, where energy deposition results are generated using MCNP6 and compared to the well-known Lockwood energy deposition experiment [8]. Specifically, 1-D energy deposition profiles are calculated for electrons incident on single- and multi-layer extended media composed of materials from beryllium to uranium. Electron pencil-beam sources were simulated with energies up to 1-MeV and angles of incidence up to 60 degrees off-normal.

Two input parameters impacting the accuracy and efficiency of the default electron transport algorithm, a class I condensed history (CH) algorithm [9], are studied. These include the number of substeps per energy step and the energy-straggling logic. Several comparisons are performed among these options.

In the following sections, the key features of the MCNP6 electron transport algorithms are summarized. The Lockwood energy deposition experiment is briefly described and details from the experiment pertinent to generating the necessary MCNP6 input files are noted. Characteristics of the simulation including the geometry and materials, physics parameters, source configuration, and so forth are noted. Finally, validation results are presented with concluding remarks on the status of the validation and anticipated future work.

### MCNP6 ELECTRON TRANSPORT: KEY FEATURES

The electron physics in MCNP6 is similar to that of the Integrated TIGER Series (ITS) [10] as described by Hughes [11]. MCNP6 transports electrons by using what is referred to as the class I CH algorithm [9]. This algorithm moves particles a fixed distance to collision that is determined such that the electron transport is computationally tractable, and the underlying multiple-scattering and energy-loss straggling distributions remain valid. The details of how the steps are determined are found in Hughes' description of the algorithm [11]; however, key features of the algorithm necessary to understand the results are elucidated further below.

There are two length scales or pathlengths important to the class I CH algorithm. First, the larger of the two, the energy step, is the pathlength necessary to sample energy-loss straggling in earlier versions of the code and it remains the pathlength associated with the tabulation of the transport data (i.e. stopping powers, multiple-scattering and energy-loss straggling distribution parameters, etc.). A step is the distance required for an electron to lose about 8% of its energy in the continuous slowing down approximation (CSDA). A step is sufficiently long that the applicable multiple-scattering theory can be inaccurate if applied at the end of a full step. Therefore, the second of the two length scales or pathlengths results from dividing the step into several angular substeps. In turn, the angular distributions are evaluated at the pathlength associated with the substep. This allows an electron to be deflected along the step at the end of each substep. The number of substeps-per-step was determined empirically for each element to optimize accuracy and efficiency, and is a default setting in MCNP6. However, there are problems that may require a user to override the default number of substeps to improve accuracy (see ESTEP parameter [12]).

While the substep distance is still determined by dividing the pathlength associated with a step into substeps, in MCNP6, energy-loss straggling is no longer evaluated at the end of a step. That is, an improvement to the energy-loss straggling logic [13] allows for energy-loss straggling to be sampled on-the-fly for any energy or pathlength and is the current default in MCNP6 (input option DBCN(18)=2). Improvements in the straggling logic were motivated by artifacts in energy spectra that were apparent in geometries with small regions. The previous form of the straggling logic responsible for the artifacts is referred to as "bin-centered" treatment. "Bin-centered" treatment was the default in previous versions of MCNP and relied on equal apportioning of step-based straggled energy loss over the substeps. This option is selected by setting DBCN(18)=0. In addition, an ITS-like straggling logic was added to MCNP (input option DBCN(18)=1). Like the bin-centered treatment, the ITS-like straggling logic relies on apportioning of step-based energy loss over substeps, but the interpolation scheme is formulated differently using a "nearest-group-boundary" treatment.

In addition to the CH algorithm, a MCNP6 single-event algorithm for transporting electrons is currently available [14]. This algorithm relies on the analog DCSs characterizing electron physics (i.e. elastic scattering, inelastic scattering, excitation, bremsstrahlung, and so on), rather than the multiple-scattering and energy-loss straggling distributions utilized by the CH algorithm. The algorithm is fundamentally different in the sense that particles travel distances to collision based on exponentially distributed collision sites. Aside from using the true transport data (i.e. the analog DCS), the single-event method does not require a special boundary crossing algorithm

as a result of utilizing the correct transport mechanics. Validation results for the single-event algorithm are not included, but will be reported in subsequent reports.

The impact of both the number of substeps-per-step and the straggling logic on electron energy deposition is demonstrated below. First, additional details regarding the Lockwood experiment and the simulation characteristics are provided.

## THE LOCKWOOD EXPERIMENT

The Lockwood energy deposition experiments [8] were motivated by the presence of ambiguities in traditional methods during the early 1970s. In particular, much of the published data reported some response profile other than energy deposition or the data was normalized to agree with other available results; many results were obtained in infinite rather than semi-infinite media to simplify experimental considerations; very little data existed for source energies less than 1.0-MeV in semi-infinite slabs; and spatial resolution in experiments for semi-infinite geometries were poor near the surface.

To improve upon previous experimental measurements, Lockwood et al. employed a thin-foil calorimetric technique that did not require any stopping power corrections and eliminated the need for a window (both required by gas-filled ionization chambers) because the device could be placed in vacuo. While the new approach devised by Lockwood et al. was a great improvement, the data is still subject to experimental uncertainties (ranging from 1% to 3% [8]) and, in some cases, unclear in how one should interpret the results such that the experiment can be reproduced for the purposes of a validation.

Lockwood et al. measured energy deposited in a thin foil calorimeter, where spatial dependence was introduced by placing additional foils between the accelerator and the calorimeter foil. The spatial location of energy deposited was reported at the thickness of the front foils plus one-half of the thickness of the calorimeter. However, in some cases one finds that there is material overlap given the dimensions of the calorimeter foil and the reported spatial locations from the measurements. The foils were large enough radially to assume that dimensions orthogonal to the beam were infinite. In some cases, thin aluminum foils were placed on either side of the calorimeter to reduce thermal coupling effects, but results are assumed to be insensitive to these thin Al foils. The electron source is a collimated accelerator beam. The beam energy is reported as known to approximately 0.1% and uncertainty in the angle of incidence is reported as less than 0.5%. However, the beam width and angular spread is not reported (a beam diameter of 0.02 mm is provided in an previous report [15]). That said, the version of ITS used to generate the theoretical energy deposition profiles in Lockwood et al. was the TIGER code, the 1-D version of ITS, leading one to believe that the experimental source configuration was intended to be a pencil beam effectively.

## SIMULATION CHARACTERISTICS

Given a brief description of the experiment, the simulations reported herein are now described. It is assumed that

the geometry consists of a 1-D, semi-infinite slab with one or multiple layers of materials. Therefore, only reflected particles can leave the system. The geometry is constructed by placing several cells adjacent to one another along the axis of orientation of the beam. In this work, the cell width is problem dependent and reported in TABLE II for the single-layer problems. That is, in the beryllium simulations, the cell width was chosen to be the same width as the Be calorimeter foil ( $2.6 \times 10^{-3}$  cm) and is independent of energy. However, in the tantalum simulations, the cell width is reduced as a function of energy.

TABLE I: Simulation Characteristics for Single-Layer Validation Study.

Material	Particle Energy (MeV)	Cell Width (cm)
Be	0.3	
	0.5	$2.6 \times 10^{-3}$
	1.0	
Ta	0.3	$1.3 \times 10^{-4}$
	0.5	$2.5 \times 10^{-4}$
	1.0	$6.3 \times 10^{-4}$

In the multi-layer simulations, the cell width in the first two regions is chosen to be consistent with the theoretical results from Lockwood et al. Along with the cell thickness, information about the step size and the substeps per cell are included in TABLE II. These cells (single- or multi-layer) are

TABLE II: Simulation Characteristics for Multi-Layer Validation Study

Problem	Material	Cell Thickness (cm)
Be-Au-Be 1-MeV	Be	$6.1 \times 10^{-3}$
	Au	$7.3 \times 10^{-4}$
Al-Au-Al 1-MeV	Al	$1.7 \times 10^{-3}$
	Au	$7.3 \times 10^{-4}$

used as tally cells (the \*F8 tally was used).

It is assumed that effects resulting from differences between a true pencil beam source and the experimental source are negligible with respect to the energy deposition profile. Therefore, the electron source is assumed to be a mono-energetic, mono-directional, point source located at the left face of the slab. In each simulation,  $10^6$  electron histories were followed until they reached the default lower-energy limit (1-keV) or left the system. The default lower energy limit (1-keV) for photons was also used.

As noted above, two major input parameters were studied. The first parameter was the number of substeps per energy step. The default value is tested and modified in some cases to demonstrate the impact of increasing the default number of substeps. To do so, each material modified must contain the ESTEP parameter:

```
m1      4000.12p 1  elib 03e  estep=4
```

The second parameter studied was the impact of the energy

straggling logic discussed above. The energy straggling logic is modified by including the following line in the data card:

```
dbcn 17j N
```

where N is zero, one, or two, for the different options.

## RESULTS

The following results include a sampling of the experimental validation of the MCNP6 electron transport algorithms for energy deposition in extended media. Both single- and multi-layer simulation results are presented for electrons with energies ranging from 0.3- to 1-MeV with normal and off-normal incidence on high- and low-Z materials. In all cases, the impact of substeps-per-step and, in turn, substeps per tally cell are demonstrated along with the impact of the straggling logic.

### Single-layer problems

In this section, single-layer problems are presented for electrons from 0.3- to 1-MeV normally incident on beryllium and tantalum. In addition, an off-normal result is presented for 0.5- and 1-MeV electrons on tantalum.

Energy deposition profiles in beryllium are presented in Figs. 1 and 2. Figure 1 shows the impact of the straggling logic for electrons with various energies and the default substep setting. In beryllium, the energy deposition profile is somewhat insensitive to differences in the straggling logic with more distinguishable differences at lower energies. In general, the default straggling logic and the "bin-centered" logic tend to give better agreement than the ITS-like logic. In Fig. 2, it is shown that increasing the number of substeps does not significantly impact the calculated energy deposition for 1-MeV electrons on beryllium (here the default straggling logic is used). The same is true in beryllium for all energies and straggling logic tested.

Energy deposition profiles in tantalum are presented in Figs. 3–5. Figure 3 shows the impact of the straggling logic for electrons with various energies and the default substep setting. In tantalum, the "bin-centered" treatment (DBCN(18)=0) appears to be the most accurate for each source energy tested. At 1-MeV, subtle differences in the energy deposition profiles near the maximum can be seen for the different straggling logic options. In general, the 1-MeV results are in good agreement with experiment. At lower energies, the impact of the straggling logic on the energy deposition profile is more significant and the calculated energy deposition near the peak is noticeably high. This is mostly remedied by overriding the default substep settings. As seen in Fig. 4, increasing the number of substeps by a factor of two improves the calculated peak energy deposition. However, improvements resulting from increasing the number of substeps beyond a factor of two appear to be negligible.

Similar behavior for the off-normal results is seen in Fig. 5, where the 1-MeV results are in better agreement than at lower energies and the calculated results tend to overestimate the experimental energy deposition. Once again, increasing the number of substeps by a factor of two improves agreement

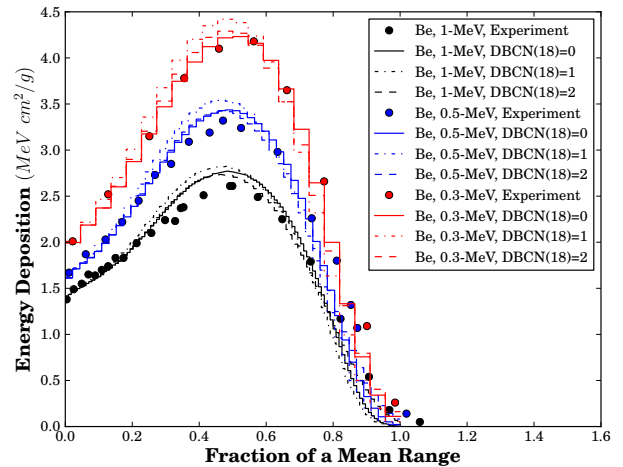


Fig. 1: Energy deposition from 0.3- to 1-MeV electrons on a 1-D, Be single-layer slab. Energy deposition profiles were generated using the default number of substeps with DBCN(18)=0, DBCN(18)=1, and DBCN(18)=2.

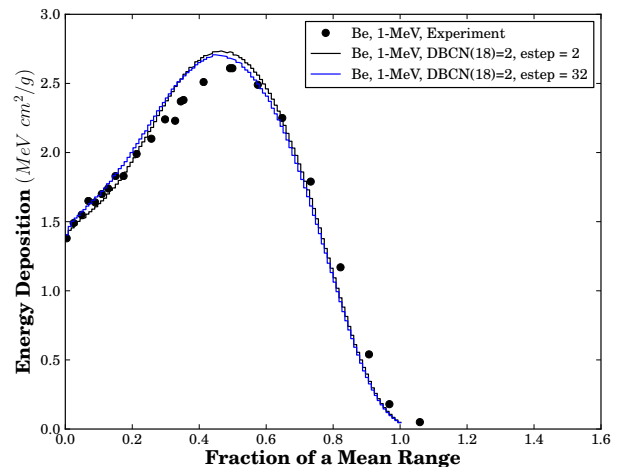


Fig. 2: Energy deposition from 0.3-MeV electrons on a 1-D, Be single-layer slab. The energy deposition profiles were generated using the default number of substeps (default is 2) and 16 times the default, and DBCN(18)=2..

with experiment. This is seen clearly in Fig. 5, where the energy deposition was calculated using the "bin-centered" logic and the number of substeps was increased from 12 to 24.

### Multilayer-layer problems

In this section, multi-layer problems are presented for 1-MeV electrons normally incident on Be-Au-Be and Al-Au-Al targets.

In Figs. 6 and 7, the impact of the various energy-straggling logic options is presented. As seen in Fig. 6, the energy deposition is overestimated in the Be regions regard-

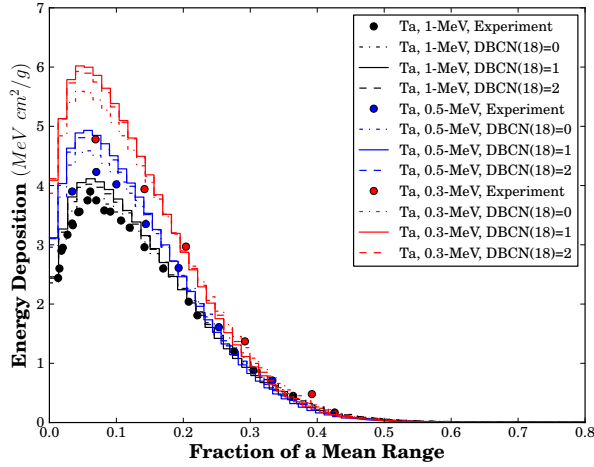


Fig. 3: Energy deposition from 0.3- to 1-MeV electrons on a 1-D, Ta single-layer slab. Energy deposition profiles were generated using the default number of substeps with DBCN(18)=0, DBCN(18)=1, and DBCN(18)=2.

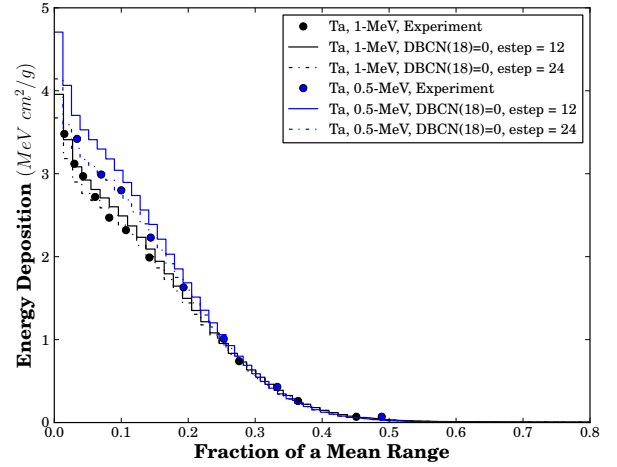


Fig. 5: Energy deposition from 0.5- and 1-MeV electrons 60 degrees off-normally incident on a 1-D, Ta single-layer slab. Energy deposition profiles were generated using an increasing number of substeps and DBCN(18)=0.

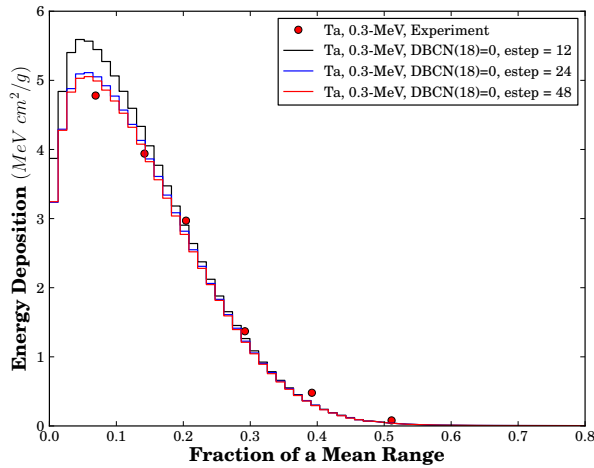


Fig. 4: Energy deposition from 0.3-MeV electrons on a 1-D, Ta single-layer slab. The energy deposition profiles were generated using an increasing number of substeps (default is 12) and using the straggling logic of DBCN(18)=0.

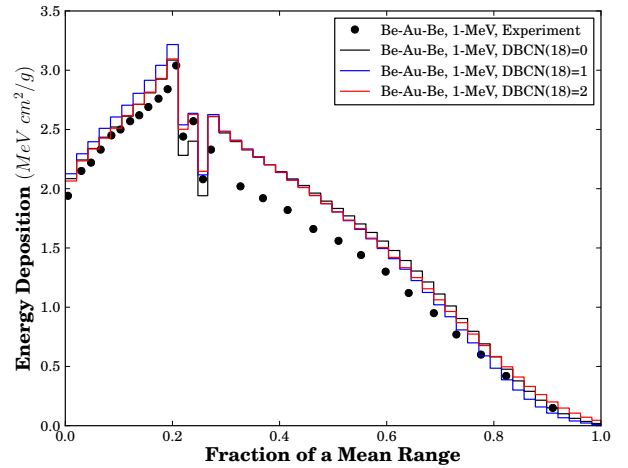


Fig. 6: Energy deposition from 1-MeV electrons on a 1-D, Be-Au-Be multi-layer slab. Energy deposition profiles are generated using DBCN(18)=0, DBCN(18)=1, and DBCN(18)=2.

less of the energy-straggling logic option, while the default logic and the ITS-like logic are in good agreement in the gold region. In Fig. 7, better agreement is seen throughout the three regions for all energy-straggling logic options.

Although the impact of the number of substeps-per-step is not included, in both multi-layer configurations the energy deposition profile is mostly insensitive to increasing the number of substeps. This implies that the disagreement is likely a result of the boundary crossing algorithm required when encountering a material interface (particularly in the Be-Au-Be configuration).

## CONCLUSIONS

A sampling of a broader MCNP6 electron-photon transport validation suite was presented. The impact of the energy-straggling logic and the number of substeps-per-step on energy deposition profiles was demonstrated. In many of the cases presented herein, the default settings resulted in energy deposition profiles that were in good agreement with experiment. There were a few cases where the default settings were insufficient and the energy-straggling logic and/or the number of substeps required modification.

The multi-layer problems demonstrated one of the well known limitations of the CH algorithm. That is, the need for

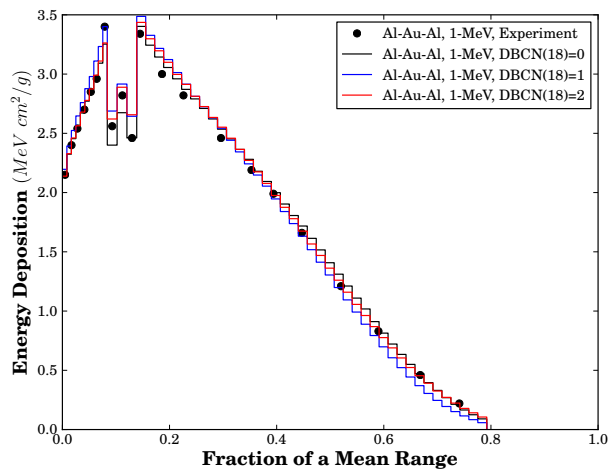


Fig. 7: Energy deposition from 1-MeV electrons on a 1-D, Al-Au-Al multi-layer slab. Energy deposition profiles are generated using DBCN(18)=0, DBCN(18)=1, and DBCN(18)=2.

a boundary crossing algorithm at material interfaces, which is an additional approximation beyond those already incurred when utilizing multiple-scattering and energy-loss straggling distributions.

It is of interest to develop guidance or best practices when using MCNP6 to calculate electron energy deposition. However, further testing must be completed to identify the optimal energy-straggling logic and "rules-of-thumb" for the minimal number of substeps-per-step, or substeps per tally cell.

## ACKNOWLEDGMENTS

This work was funded by the US Department of Energy's National Nuclear Security Administration, under Los Alamos National Security, LLC, Contract No. DE-AC52-06NA25396.

## REFERENCES

1. T. GOORLEY ET AL., "Initial MCNP6 Release Overview," *Nuclear Technology*, **180**, 298 (2012).
2. R. D. MOSTELLER, "Validation Suites for MCNP," Proc. of the American Nuclear Society Radiation Protection and Shielding Division 12th Biennial Topical Meeting, American Nuclear Society, Inc., La Grange Park, IL 60526 USA (2002).
3. R. D. MOSTELLER, F. B. BROWN, and B. C. KIEDROWSKI, "An Expanded Criticality Validation Suite for MCNP," Proc. Int. Conf. on Nuclear Criticality, Edinburgh, Scotland, September 19 - 22, 2011, <http://www.informaglobalevents.com/event/icnc2011> (2011).
4. B. C. KIEDROWSKI ET AL., "MCNP6 Shielding Validation Suite: Past, Present, and Future," *Trans. Am. Nucl. Soc.*, **105**, 559–561 (2011).
5. D. J. WHALEN, D. E. HOLLOWELL, and J. S. HENDRICKS, "MCNP: Photon Benchmark Problems," Tech. Rep. LA-12196, Los Alamos National Laboratory (1991).
6. D. P. GIERGA and K. J. ADAMS, "Electron/Photon Verification Calculations Using MCNP4B," Tech. Rep. LA-13440, Los Alamos National Laboratory (1999).
7. P. L. LIBBY, H. G. HUGHES, and J. T. GOORLEY, "Electron Transmission and Backscatter Verification Calculations Using MCNP5," Tech. Rep. LA-UR-03-5751, Los Alamos National Laboratory (2003).
8. LOCKWOOD ET AL., "Calorimetric Measurement of Energy Deposition in Extended Media — Theory vs Experiment," Tech. Rep. SAND-0414-UC-34a, Sandia National Laboratory (1987).
9. M. J. BERGER, "Monte Carlo Calculation of the Penetration and Diffusion of Fast Charged Particles," in B. ALDER, S. FERNBACH, and M. ROTENBERG, editors, "Methods in Computational Physics," Academic Press, vol. 1, pp. 135–215 (1963).
10. T. W. LAUB ET AL., "The Integrated TIGER Series version 5.0," *Trans. Am. Nucl. Soc.*, **95**, 754–755 (2006).
11. H. G. HUGHES, "Treating Electron Transport in MCNP," Tech. Rep. LA-UR-96-4583, Los Alamos National Laboratory (1996).
12. X-5 MONTE CARLO TEAM, "MCNP - A General N-Particle Transport Code, Version 5 - Volume I: Overview and Theory," Tech. Rep. LA-UR-03-1987, Los Alamos National Laboratory (2003).
13. H. G. HUGHES, "Improved Logic for Sampling Landau Straggling in MCNP5," Tech. Rep. LA-UR-05-4404, Los Alamos National Laboratory (2005).
14. H. G. HUGHES, "Recent Developments in Low-Energy Electron/Photon Transport for MCNP6 - Revision 4," Tech. Rep. LA-UR-12-24213 rev 4, Los Alamos National Laboratory (2013).
15. G. J. LOCKWOOD, G. H. MILLER, and J. A. HALBLEIB, "Electron Energy Deposition in Multilayer Geometries," *IEEE Trans. Nucl. Sci.*, **NS-23**, 6, 1862–1866 (1976).